




Article

Evaluation of the Effect of the Vigor of Soybean Seeds Treated with Micronutrients Using X-ray Fluorescence Spectroscopy and Hyperspectral Imaging

Rafael Mateus Alves ^{1,*}, Francisco Guilhien Gomes-Junior ¹, Abimael dos Santos Carmo-Filho ¹, Glória de Freitas Rocha Ribeiro ¹, Carlos Henrique Queiroz Rego ¹, Fernando Henrique Iost-Filho ², and Pedro Takao Yamamoto ²

¹ Department of Crop Science, “Luiz de Queiroz” College of Agriculture (ESALQ), University of São Paulo (USP), Piracicaba 13418-900, Brazil; francisco1@usp.br (F.G.G.-J.); abimaelfilho@usp.br (A.d.S.C.-F.); glorinharribeiro@usp.br (G.d.F.R.R.); chqragro@usp.br (C.H.Q.R.)

² Department of Entomology and Acarology, ESALQ, University of São Paulo (USP), Piracicaba 13418-900, Brazil; fernandohiost@usp.br (F.H.I.-F.); pedro.yamamoto@usp.br (P.T.Y.)

* Correspondence: rafaelmateusalves@usp.br

Abstract: Seed treatment with micronutrients is a crucial strategy for providing early seedling supply during development, and is commonly employed in soybean cultivation. However, responses to micronutrient treatment may vary based on seed vigor levels. Therefore, this study aimed to assess the potential of hyperspectral imaging combined with preprocessing and machine learning, compared to X-ray fluorescence spectroscopy, in evaluating the dynamics of micronutrient uptake during the germination of soybean seeds with varying levels of vigor. Two seed lots with differing levels of vigor were utilized for the analysis. The absorption of micronutrients by the seeds was evaluated using X-ray fluorescence spectroscopy (XRF), microprobe X-ray fluorescence spectroscopy (μ -XRF) and hyperspectral imaging (HSI) in two regions of interest (cotyledons and the embryonic axis). Artificial neural network (ANN), decision tree (DT) and partial least squares–discriminant analysis (PLS-DA) classification models, along with the Savitzky–Golay (SG), standard normal variation (SNV) and multiplicative scatter correction (MSC) methods, were employed to determine seed vigor based on the impact of micronutrient treatment. XRF identified higher concentrations of micronutrients in the treated seeds, with zinc being the predominant element. μ -XRF analysis revealed that a significant proportion of the micronutrients remained adhered to the hilum and seed coat, irrespective of seed vigor. The PLS-DA classification model using spectral data exhibited higher accuracy in classifying soybean seeds with high and low vigor, regardless of seed treatment with micronutrients and the analyzed region.

Keywords: *Glycine max*; seed physiological potential; seed coating; nutrient uptake; machine learning



Citation: Alves, R.M.; Gomes-Junior, F.G.; Carmo-Filho, A.d.S.; Ribeiro, G.d.F.R.; Rego, C.H.Q.; Iost-Filho, F.H.; Yamamoto, P.T. Evaluation of the Effect of the Vigor of Soybean Seeds Treated with Micronutrients Using X-ray Fluorescence Spectroscopy and Hyperspectral Imaging. *Agronomy* **2023**, *13*, 1945. <https://doi.org/10.3390/agronomy13071945>

Academic Editors: Silvia Arazuri and Baohua Zhang

Received: 3 June 2023

Revised: 24 June 2023

Accepted: 28 June 2023

Published: 23 July 2023



Copyright: © 2023 by the authors. Licensee MDPI, Basel, Switzerland. This article is an open access article distributed under the terms and conditions of the Creative Commons Attribution (CC BY) license (<https://creativecommons.org/licenses/by/4.0/>).

1. Introduction

Soybean (*Glycine max* (L.) Merrill) is the most economically and nutritionally important legume in the world; its grains contain approximately 40% protein and 20% lipids [1], highlighting its economic and nutritional relevance as a direct source of food and a raw material for the production of animal-based foods. The global demand for food will continue to grow, and Brazil is a major player with the potential to meet this need, given its availability of suitable land for grain production and appropriate technologies for cultivation under tropical conditions. However, the challenge will be to maintain soybean production capacity in a profitable and sustainable way [2]. In this sense, the use of superior-quality seeds is an efficient way to meet the challenge of increasing food demand [3].

To be considered of high quality, soybean seeds must have high germination, vigor and sanitation rates, in addition to possessing physical and genetic purity. Seeds with

these characteristics result in high-performance seedlings, which establish more easily in environments with adverse biotic and abiotic conditions, with greater speed of emergence and plant development. However, seeds with low or medium vigor produce weak seedlings, with little competitiveness in field establishment [4]. Thus, the seed is the most important raw material for agriculture, because it will determine the development and proper establishment of plants in the field.

Increased crop production can be achieved using production technologies associated with the use of high-quality seeds. In this context, the use of micronutrients through seed treatment stands out as it makes microelements available for the process of seed germination and initial plant development. Essential micronutrients such as zinc (Zn), copper (Cu), molybdenum (Mo) and manganese (Mn) are examples of elements required in small amounts by plants, and together or in isolation, they act in biochemical processes necessary for the proper development of the plant, influencing productivity [5]. Micronutrients are involved in virtually all biochemical and physiological functions [6]. However, there is limited information on the use of micronutrients in seed treatment in relation to physiological potential and their effects on early plant development.

The use of efficient techniques to quantify the micronutrients made available through seed treatment is indispensable in elucidating the dynamics of the uptake and utilization of micronutrients by seeds during germination and initial plant development. The X-ray fluorescence spectroscopy (XRF) technique stands out in the study of the elemental composition of plant tissues as it allows for *in vivo* analyses, due to its non-destructive characteristics and minimal sample preparation, in addition to its ability to simultaneously evaluate more than one chemical element in the same sample [7]. The efficiency of the XRF technique has already been confirmed in the evaluation of soybean seed treatment with Cu, Mo and Zn [8], and it has been shown to be a promising technique for the evaluation of soybean seed treatment for improving vigor, being able to clarify the process of the absorption and translocation of micronutrients during the germination process [9].

However, the use of other complementary techniques that allow for accurate seed evaluations provides greater assurance in decision making. Hyperspectral imaging (HSI) provides a dataset (hypercube) that comprises hundreds of spectra distributed over the analyzed area [10]. Spectral information can be used in the rapid assessment of seed quality by integrating spectral and spatial information, assisting in capturing structural or chemical composition changes [11]. Spatial and spectral processing of HSI must be used to minimize the effect of factors affecting spectral measurement. Spatial processing is associated with the selection of the region of interest (ROI) to be analyzed. For example, a soybean seed may have as its ROI the region of the embryonic axis and cotyledons. Meanwhile, spectral processing aims to avoid the influence of undesirable factors. These factors can be due to light scattering, particle size effects, differences in morphology, porosity, roughness and detectors [12].

The amount of data obtained through HSI needs to be analyzed in order to extract useful and meaningful information from the images. Multivariate statistical analysis stands out as a tool capable of reducing the dimensionality of the data, retaining essential spectral information. Principal component analysis (PCA) is one of the most useful multivariate techniques in HSI analysis [10]. In PCA, the original variables are linearly combined into principal components, which condense most of the information into a few variables, decreasing the dimensionality of the database without the significant loss of chemical information [13].

In addition, for HSI data analysis, many soybean seed researchers have applied data preprocessing and machine learning algorithms, such as Savitzky–Golay (SG) preprocessing coupled with support vector machine (SVM) models for discriminating seed viability [14], MSC in conjunction with ensemble learning (EL) for soybean variety identification [15], SG and MSC with the partial least squares discrimination analysis (PLS-DA) method for fatty acid content classification in soybean seeds [16], SNV associated with partial least squares regression (PLSR) methods for predicting protein content [17], MSC with a one-dimensional

convolutional neural network for identifying soybeans with high oil content [18], and the use of spectra without preprocessing with a PLSR model for determining soybean seed moisture content [19].

However, no work has been found in the literature that uses the HSI technique with preprocessing and models to evaluate the metabolism of soybean seeds showing different levels of vigor and subjected to micronutrient treatment. Thus, the objective of this work was to explore the potential of the hyperspectral imaging technique combined with preprocessing and machine learning in comparison with X-ray fluorescence spectroscopy in the evaluation of the dynamics of micronutrient uptake during the germination of soybean seeds with different levels of vigor.

2. Materials and Methods

2.1. Seed Material and Classification of Vigor

This research was carried out using two lots of soybean seeds of the cultivar M5917 IPRO, using a sieve of 6.5 mm; the seeds had two levels of vigor, both with germination higher than 80%, the standard required for commercialization of seeds, established by the Ministry of Agriculture, Livestock and Food Supply. With the intention of characterizing the seed lots, evaluations of water content, a standard germination test, a first germination count [20], accelerated aging assessment, a tetrazolium test [21] and an assessment of seedling emergence in the field were performed. All tests were conducted with 8 repetitions of 50 seeds per lot.

2.2. Evaluation of the Uptake of Micronutrients by Seeds

2.2.1. Imbibition Curve

The soaking curve was determined using four repetitions of 50 seeds per lot. Initially the water content of the seeds was determined; then, the repetitions of each lot were weighed on a scale with a precision of 0.0001 g and distributed on paper towels, moistened with water equivalent to 2.5 times the dry mass of the paper, and kept in a germinator regulated at 25 °C in the absence of light [20]. To calculate the water content throughout the soaking process, the seeds were removed from the paper towel roll and weighed at one-hour intervals for 48 h. The criterion for germination was the protrusion of the primary root (≥ 2 mm) of 50% of the seeds of each lot. The results are expressed as a percentage of water content, were calculated using Equation (1) and were used to plot the soaking curve for each batch.

$$WC (\%) = \left(\frac{fm - fi}{fi} \right) \times 100 \quad (1)$$

where WC represents the percentage of water content (%), fm represents the final mass and fi represents the initial weight.

2.2.2. Seed Treatment

The seeds from each lot were treated with the commercial product ADB 307—Broadacre Black[®], containing the following micronutrient quantities: 15.1% Zn, 9.4% Mn, 6.7% Cu and 3.2% Mo. We used the manufacturer's recommended dose (4 g of the product per kg of seeds), and the control treatment did not receive any treatment (0 g of micronutrient per kg of seeds). The seed treatment was performed using a plastic bag with a capacity of 1 kg, where five hundred grams of seeds were inserted, and then, using a syringe, the respective dose of the product was added. The plastic bag was shaken manually and constantly for two minutes. Following this, the seeds were spread on plastic trays and kept in a laboratory environment for drying; afterwards, they were stored in labeled paper kraft bags until the experiment was conducted.

2.2.3. Analysis of Micronutrient Uptake via X-ray Fluorescence Spectroscopy (XRF)

The evaluation of micronutrient absorption (Cu, Mn, Mo and Zn) by the treated seeds was conducted with four repetitions of 50 seeds of each lot per dose, placed in paper towels

moistened with water equivalent to 2.5 times the dry mass of the paper. The rolls were kept in a germinator at 25 °C for 20 h. After the soaking period, the tegument of each seed was removed manually to eliminate excess product. Subsequently, the seeds were dried in an oven at 60 °C for 72 h [22]. The dried seeds were ground using an IKA® A10 mill, and then, the obtained material was passed through a sieve with an opening of 500 µm. After being ground and sieved, the samples were weighed on a scale with 0.001 g precision, and 5 g were placed in a 23 mm internal diameter polyethylene container covered with 6 µm thick polypropylene film.

The analyses were performed using an energy-dispersive X-ray fluorescence spectrometer—EDXRF (Shimadzu® EDX-720, Kyoto, Japan). The samples were irradiated in a Rh X-ray tube operated at 30 kV. The current was adjusted automatically (maximum 1 mA). A 10 mm collimator was chosen. Detection was carried out on a Si (Li) detector cooled with liquid nitrogen. The intensity of the K α element counts per second (cps/µA) was obtained via deconvolution of the sample's X-ray spectrum using the Shimadzu EDX software package. To calibrate the data obtained for soaked soybeans via the EDXRF method, a calibration curve was produced with the data obtained using the atomic absorption spectroscopy technique (AAS) on the same samples. The results are expressed as the concentration of the elements (mg per kg of seeds).

2.2.4. Analysis of Micronutrient Uptake via Microprobe X-ray Fluorescence Spectroscopy (μ -XRF)

The evaluation of the absorption of micronutrients (Cu, Mn, Mo and Zn) by the treated seeds was conducted with eight seeds of each lot per dose. The dose recommended by the manufacturer (4 g per kg of seeds) and the control with 0 g per kg of seeds were used. The absorption of micronutrients was evaluated in the seeds after 20 h of soaking. After the soaking period, the seeds of each lot and dose were cut longitudinally through the center of the embryonic axis using a blade, exposing its central cylinder. A cotyledon from each seed was fixed on an acrylic plate using double-sided tape.

The investigation of micronutrients in seeds was performed using an X-ray microprobe spectrometer (μ -XRF) (M4 Tornado®, Bruker, Mannheim, Germany), operated with a Rh X-ray tube at 50 kV and 600 µA, under a 20 mbar vacuum, without filters, and with a 25 µm polycapillary X-ray beam. The cotyledon was analyzed in the region of the tegument, in the periphery of the cotyledon, in the center of the cotyledon and in the hilum using a scan line with a distance between the points of 25 µm. The evaluations of the embryonic axis were performed at four points (one point in the region of the root meristem, two points in the region of the hypocotyl, one in a position closer to the radicle and the other closer to the region of the plumule meristem, and another point in the plumule meristem), as shown in Figure 1. The analysis time at each point was 10 s. The results are expressed as a mass percentage of the elements of interest (Cu, Mn, Mo and Zn), taking into account the percentage of other elements (K, P, Ca, Fe and S) present in the seed.

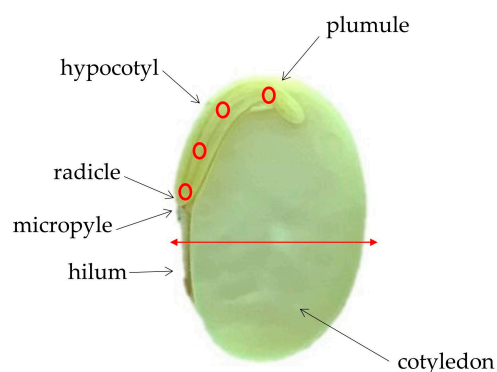


Figure 1. Schematic representation of the points and scan line (in red color) for μ -XRF analysis in soybean seeds.

2.2.5. Statistical Analysis

The data obtained from X-ray fluorescence spectroscopy (XRF) analysis were subject to presuppositions based on normality and homogeneity of residual variances. The analysis of variance was formulated using the F test ($p < 0.05$). Where significant variance was observed in the analysis, the complementary Fisher's Least Significant Difference (LSD) test ($p < 0.05$) was applied. The data from the microprobe X-ray fluorescence spectroscopy (μ -XRF) were analyzed using descriptive statistics (minimum, maximum, first quartile, third quartile, median and outliers). All analyses were performed using R software version 4.2.3 [23]. The software libraries 'EspDes.pt' and 'ggplot2' were used.

2.3. Hyperspectral Imaging System

2.3.1. Sample Preparation

The acquisition of hyperspectral images of seeds treated with micronutrients included 50 seeds from each lot per dose, placed on paper towels moistened with water equivalent to 2.5 times the dry mass of the paper. The rolls were kept in a germinator at 25 °C for 20 h. After the soaking period, the treated seeds from each repetition were cut longitudinally through the center of the embryonic axis using a blade, exposing its central cylinder. The halves were opened and fixed on acrylic plates using double-sided tape. For each seed, two regions of interest were selected (cotyledons and the embryonic axis), from which the spectral reflectance was recorded.

2.3.2. Hyperspectral Image Acquisition

A hyperspectral pushbroom spectral camera (PIKA L, Resonon Inc., Bozeman, MT, USA) equipped with a 23 mm objective lens was used to capture spectral reflectance (Figure 2). The camera operates in the wavelength range of 400 to 1000 nm (Spectral Range), consisting of 281 bands (spectral channels) with a spectral resolution of 3 nm (spectral resolution) and a spectral bandwidth of 2.1 nm (spectral bandwidth). Each line of the camera captures 900 spatial pixels. The data collection took place in a dark room illuminated by artificial lighting. A tower was used to mount 15 W, 12 V LED light bulbs arranged in two angled rows on either side of the lens, with two bulbs in each row. To ensure a stable power supply, a voltage stabilizer (Type PR-7b, Tripp-Lite, Chicago, IL, USA) was employed for the lighting system. White calibration was performed using a polyethylene plastic board (Type 822, Spectronon Pro, Resonon, Bozeman, MT, USA), while dark calibration was achieved by covering the lens. By comparing the recorded reflectance of the samples against the white and dark calibration, the relative reflectance of each seed's regions of interest, specifically the cotyledons and embryonic axis, could be calculated. To minimize the impact of data drift on subsequent modeling, the original spectra of the soybean seed regions of interest underwent preprocessing.

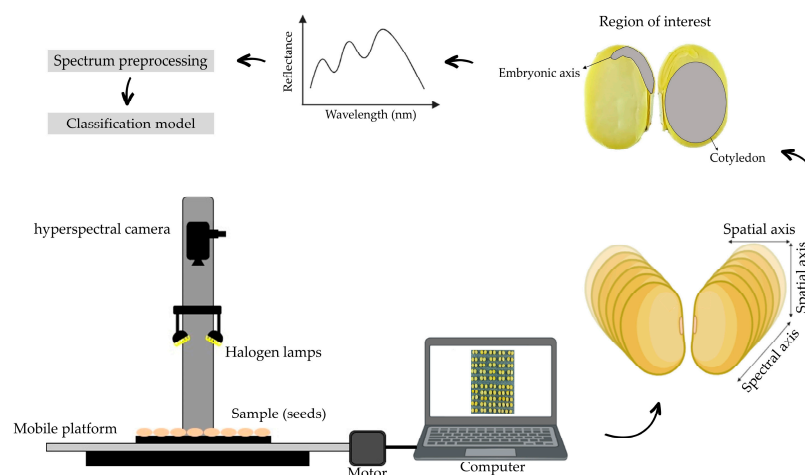


Figure 2. Hyperspectral image acquisition system.

2.3.3. Spectral Preprocessing

This step consists of eliminating noise introduced during the image acquisition process. Therefore, preprocessing the spectral data can highlight valid information and improve the accuracy of the classification model. Overall, multiplicative scatter correction (MSC) improves the signal-to-noise ratio of the spectrum by enhancing the spectral information [24]. Standard normal variation (SNV), on the other hand, is used to reduce the effects of particle surface inhomogeneity and scattering [25]. In this study, spectral preprocessing of multiplicative scatter correction (MSC) and standard normal variation (SNV) was used on data in regions of interest (cotyledons and embryonic axis) of soybean seeds with different levels of vigor that were untreated (0 g per kg of seeds) and treated with micronutrients (4 g per kg of seeds).

2.3.4. Optimal Wavelength Selection

The wavelength range of the original spectrum was 384.7–1021.7 nm (300 bands). For the analysis in this study, the first and last spectral bands were omitted from each data file as they were considered noise, and wavelengths between 400 and 1000 nm (281 bands) were adopted. Principal component analysis (PCA) is an unsupervised clustering technique used for feature extraction and pattern recognition without prior knowledge of the data. In this study, PCA was performed on raw and preprocessed spectral data from regions of interest (cotyledons and embryonic axis) of soybean seeds with different levels of vigor that were untreated (0 g per kg of seeds) and treated with micronutrients (4 g per kg of seeds). Through PCA, the 28 best-ranked bands out of the 281 bands were selected as a function of the contribution of each variable. These 28 bands represent about 10% of the total bands. Subsequently, these bands were used in the classification model.

2.3.5. Evaluation of the classification model

Machine learning approaches using an artificial neural network (ANN), a decision tree (DT) and partial least squares–discriminant analysis (PLS-DA) were employed to analyze hyperspectral data and generate classification models to identify the vigor of soybean seeds subjected to micronutrient treatment. The regions studied were the cotyledons and embryonic axis based on different methods of preprocessing (Section 2.3.3) and wavelength selection (Section 2.3.4). For the construction of the ANN, DT and PLS-DA models, the dataset was randomly divided into two parts: 70% was used for training, and the remaining 30% was used for testing. Additionally, the categorical matrix contained artificial values of 0 and 1, where 0 corresponded to the untreated group and 1 to the treated seed group. In the ANN model, the following hyperparameters were considered: the number of hidden layers (2), the number of neurons in the hidden layers (20 and 10), the learning rate (adaptive) and the activation function (ReLU). For the DT model, the hyperparameters *n*tree and *m*try were set to 500 and 30, respectively. In the PLS-DA model, the number of components used was the default, and no cross-validation was performed.

The performance of the models was evaluated based on accuracy, as defined in Equation (2). Higher accuracy indicates better predictive performance of the model. The data processing software used was R version 4.2.3 [23]. The software libraries ‘neuralnet’, ‘rpart’ and ‘pls’ were utilized for the analysis.

$$Ac = \left(\frac{TP + TN}{TP + FN + TN + FP} \right) \quad (2)$$

In Equation (2), *Ac* represents the accuracy, *TP* represent true positives (the number of correctly identified positive samples), *TN* indicate true negatives (the number of correctly identified negative samples), *FN* represent false negatives (the number of incorrectly identified negative samples) and *FP* indicate false positives (the number of incorrectly identified positive samples).

3. Results

3.1. Classification of Vigor

Based on the initial characterization of the seed lots, water content values of 7.5% and 7.8% were observed for the high- and low-vigor lots, respectively. Analysis of variance indicated significant differences (as determined by the F-test) for the germination (G), first germination count (FGC), accelerated aging (AA), tetrazolium vigor (TZ) and field emergence (FE) tests (Figure 3). It is noteworthy that both lots exceeded the minimum germination requirement set for commercial soybean seeds ($\geq 80\%$). Based on these results, the seed lots were classified as having high and low vigor for the purpose of this research.

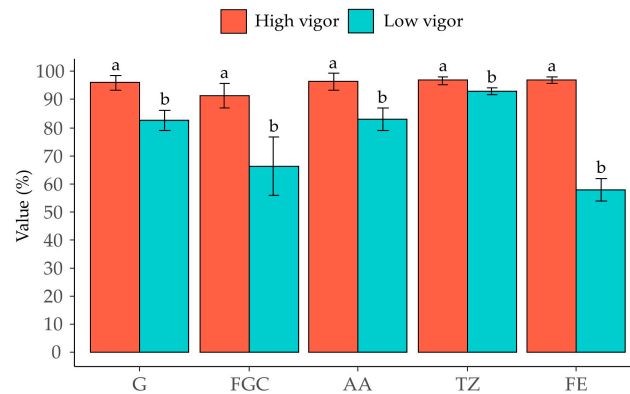


Figure 3. Standard tests result for physiological potential classification of soybean seed lots. Germination (G), first germination count (FGC), accelerated aging (AA), tetrazolium vigor (TZ) and field emergence (FE). All samples showed statistical differences between groups, significant at 5% probability according to F-test ($p < 0.05$). a and b indicate the statistical difference between the lots.

3.2. Evaluation of the Uptake of Micronutrients by Seeds

As observed in Figure 4, during the first 12 h in contact with the moist substrate, the seeds exhibited rapid hydration. Subsequently, there was an intermediate phase characterized by slower absorption. The seeds from the high-vigor lot had a higher water content throughout the 48 h imbibition period compared to the low-vigor lot (Figure 4). Additionally, there was a difference of approximately eight hours in the protrusion of the primary root in 50% of the seeds between the high-vigor lot (28 h) and the low-vigor lot (36 h). A soaking period of 20 h was adopted for the analysis of micronutrient absorption in the seeds from lots 1 and 2. Within this timeframe, primary root protrusion had not yet occurred for both seed lots.

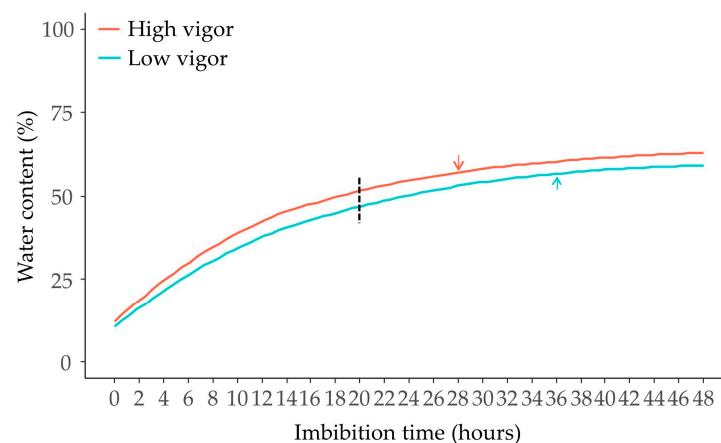


Figure 4. Water uptake by soybean seeds during the first 48 h of germination, from both high- and low-vigor seed lots. Arrows indicate 50% primary root protrusion (≥ 2 mm) for each lot, and the dotted line corresponds to the time when micronutrient uptake analyses were performed.

Using the X-ray fluorescence technique, it was not possible to quantify molybdenum (Mo) in the seeds, which can be attributed to its low concentration (3.2%) in the utilized product. Figure 5 presents the results of micronutrient concentration in the seeds after 20 h of imbibition. Significant differences were observed between the seeds from the high- and low-vigor lots, with the high-vigor lot exhibiting higher concentrations. Even without micronutrient treatment (0 g per kg of seeds), the seeds showed considerable concentrations of Cu (12.37 and 11.14 mg per kg of seeds), Mn (24.75 and 19.44 mg per kg of seeds), and Zn (44.11 and 34.69 mg per kg of seeds), respectively. Zn exhibited the highest concentration, followed by Mn and Cu, respectively, for both lots. However, when treated with micronutrients (4 g per kg of seeds), there was no significant difference between the seeds from both lot. Nevertheless, it is worth noting that the concentrations of micronutrients in the seeds increased, with Zn showing a nearly tripling effect (Figure 5b). This behavior may be related to the higher concentration of Zn (15.1%) in the utilized product.

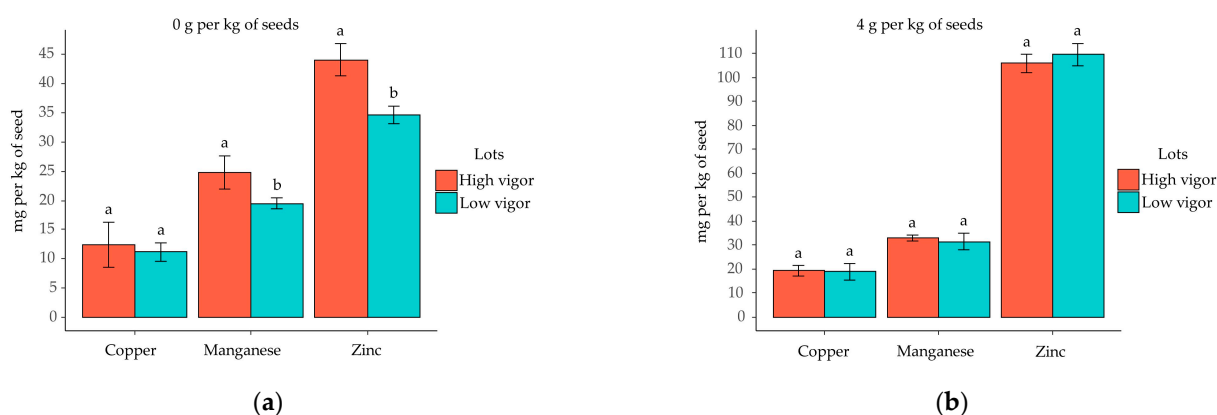


Figure 5. (a,b) Concentration of copper, manganese and zinc in soybean seeds of two lots treated with doses of micronutrients and analyzed via XRF. a and b indicate significant differences between the lots at 5% probability according to the F-test ($p < 0.05$).

The results of the scanned line analyzed using μ -XRF technique in the region of the seed coat, the periphery of the cotyledon, the center of the cotyledon and the hilum in seeds soaked for 20 h without micronutrient treatment (0 g per kg of seeds) and with micronutrient treatment (4 g per kg of seeds) in high-vigor seed lots (Figure 6a,b) and low-vigor seed lots (Figure 6c,d) can be explained based on the seed hydration process. When analyzing the scanned line for the dose of 0 g per kg of seeds, a low concentration (mass %) of the target elements (Cu, Mn and Zn) was observed for both lots (Figure 6a,c), confirming the findings from the XRF analysis in Figure 5a. When the seeds were treated with the dose recommended by the manufacturer (4 g per kg of seeds), it was observed for both lots that the hilum and seed coat regions exhibited the highest percentages of the elements, respectively. These results indicate that only a small amount of the elements applied through seed treatment were transferred to the interior of the cotyledons during the imbibition process. The comparative analysis of the percentage graphs of Cu, Mn and Zn for the dose of 4 g per kg of seeds (Figure 6a,d) reveals that there was no difference between the high- and low-vigor lots, as also observed in the XRF analyses (Figure 5b).

The investigation of the percentage of the microelements Cu, Mn and Zn at the analyzed points in the embryonic axis of soaked seeds without micronutrient treatment (0 g per kg of seeds) revealed low concentrations, with Zn being the microelement with the highest percentage in both lots (Figure 7a). After treatment with micronutrients at a dose of 4 g per kg of seeds, a small increase in Cu, Mn and Zn was observed in both the high- and low-vigor lots (Figure 7b). The presence of outliers was observed when the seeds received treatment. The data also revealed higher maximum values (longer tails) for the concentrations of Zn in the embryonic axis of seeds from the low-vigor lot when the dose of 4 g per kg of seeds was applied. The observed response for Zn can be attributed to its

higher concentration in the product used for seed treatment (15.1%). It is worth noting that the concentration of Zn, Mn and Cu in the embryonic axis was very low in seeds from both lots when compared to the concentrations measured in the seed coat (Figure 6b,d).

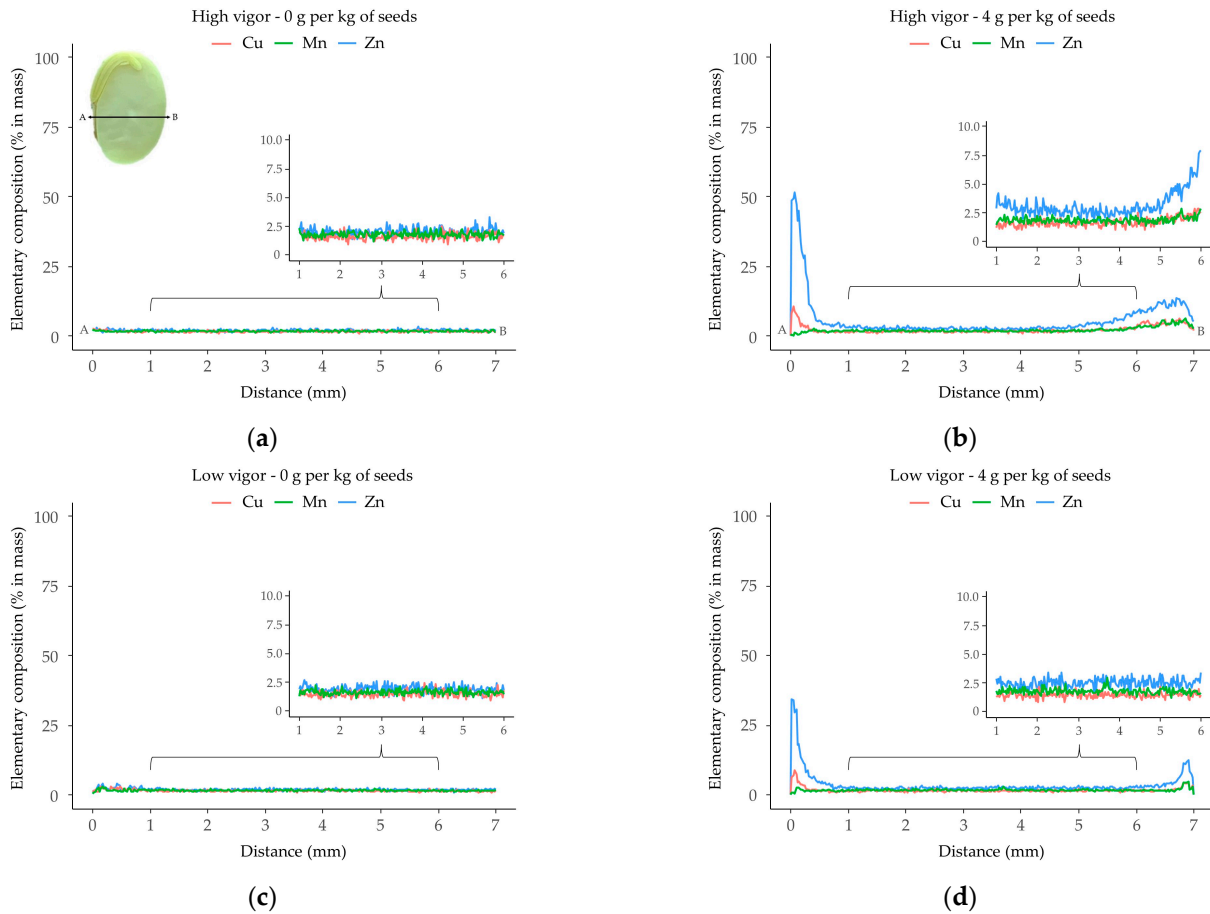


Figure 6. Average elemental composition (% in mass) measured via μ -XRF (scan line) in soybean seeds of high (a,b) and low (c,d) vigor after treatment with micronutrients at doses of 0 and 4 g per kg of seeds.

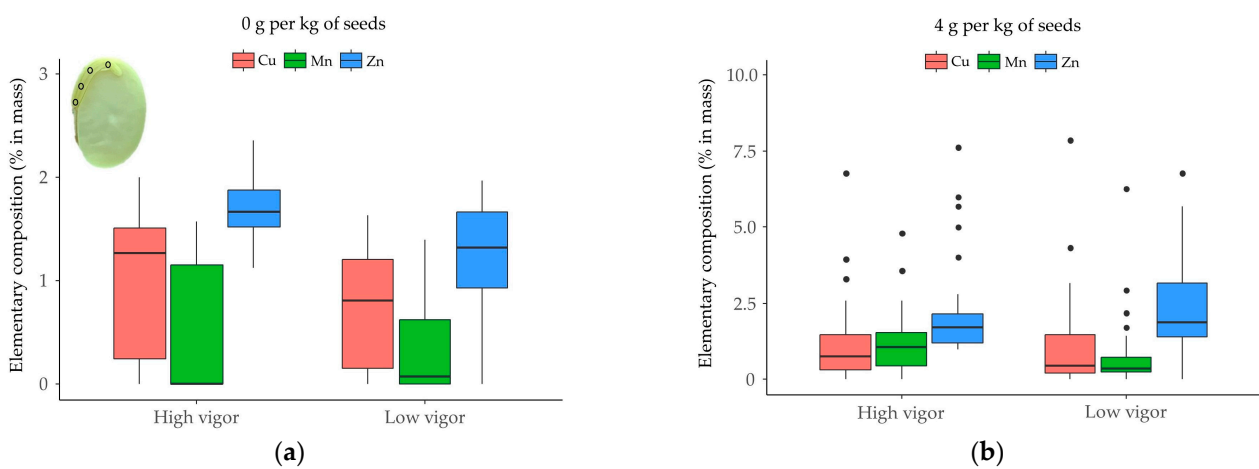


Figure 7. Average elemental composition (% in mass) measured via μ -XRF at four points on the embryonic axis of soybean seeds of high and low vigor after treatment with micronutrients at doses of 0 (a) and 4 (b) g per kg of seeds. The ends of the vertical line for each dose represent the highest and lowest values, and the symbol “•” indicates the presence of outliers.

3.3. Spectral Data Analysis

The average spectral curves of the raw data corresponding to micronutrient doses of 0 and 4 g per kg of seeds from the cotyledon region (Figure 8a,b) and embryonic axis (Figure 8c,d) of the high- and low-vigor lots are displayed below, respectively. The cotyledon region and embryonic axis of the seeds from the low-vigor lot that were not treated with micronutrients (0 g per kg of seeds) exhibited higher reflectance (Figure 8a,c) in the visible (400–700 nm) and near-infrared (700–940 nm) regions. In the cotyledon region and embryonic axis of seeds treated with the dose of 4 g per kg of seeds, no difference in reflectance was observed between the high- and low-vigor lots. The relationship between seed vigor and reflectance of the internal region of soybean seeds is not yet well-established in the context of seed physiology. However, it has been observed that less vigorous seeds, regardless of the analyzed region, exhibit higher reflectance in the near-infrared range (700–940 nm). This suggests that the reflectance properties of the internal region may be influenced by seed vigor, particularly due to the seeds' water content (Figure 4).

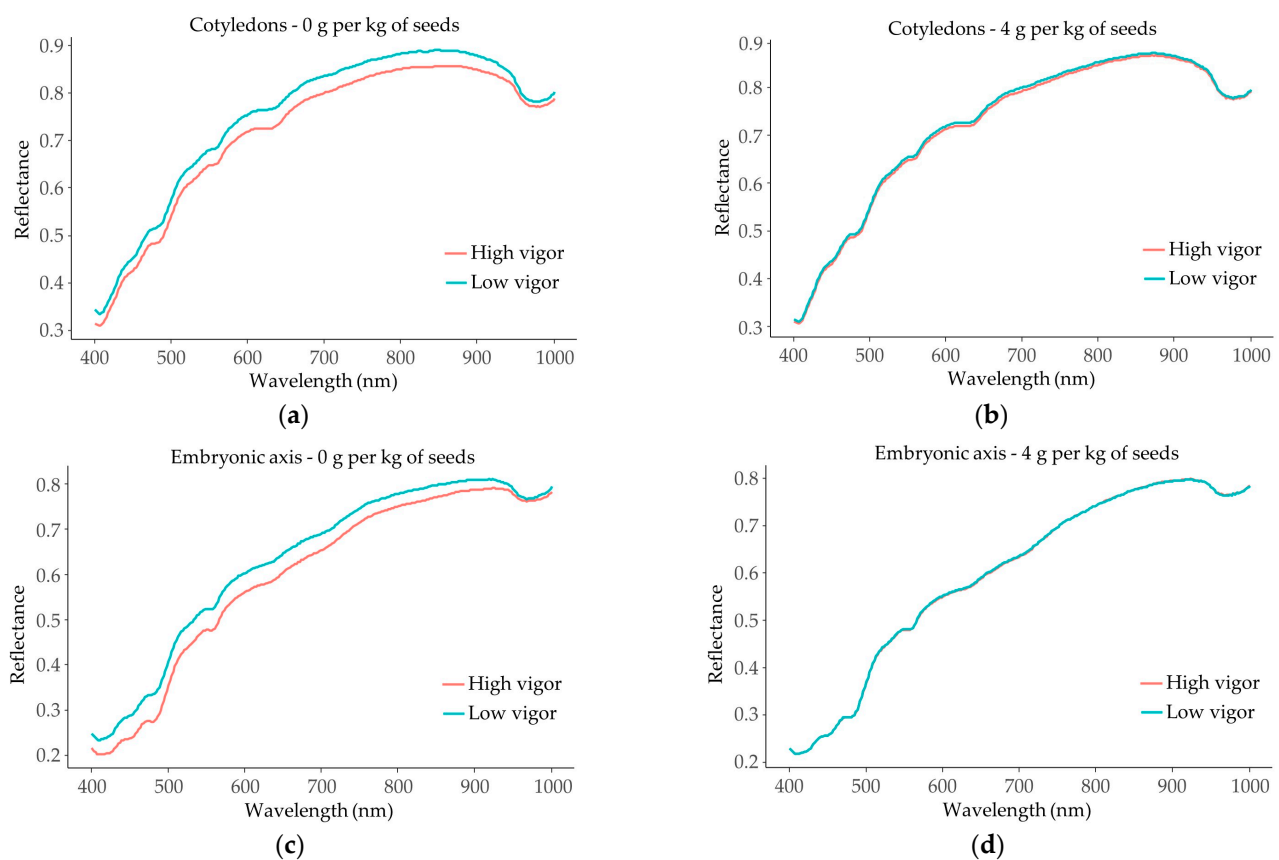


Figure 8. Average spectral curves of the cotyledon (a,b) and embryonic axis (c,d) regions of soybean seeds from the high-vigor lot and the low-vigor lot, both untreated (a,c) and treated (b,d) with micronutrient dose and soaked for 20 h.

The raw spectral information of the cotyledon region of untreated (0 g per kg of seeds) and micronutrient-treated (4 g per kg of seeds) soybean seeds from the high- and low-vigor lots is shown in Figure 9a,b, respectively. The applied preprocessing techniques, MSC and SNV, can be observed in Figure 9c–f, respectively. The comparison of the raw and processed spectral profiles of the cotyledon region in soybean seeds from the high- and low-vigor lots shows that the applied processing methods have reduced spectral noise, resulting in smoother spectral curves. By analyzing the entire studied range (400–1000 nm), it can be observed that the spectral trends after processing using the MSC and SNV methods were similar in the cotyledon region of both untreated (0 g per kg of seeds) and micronutrient-treated (4 g per kg of seeds) seeds from the high- and low-vigor lots.

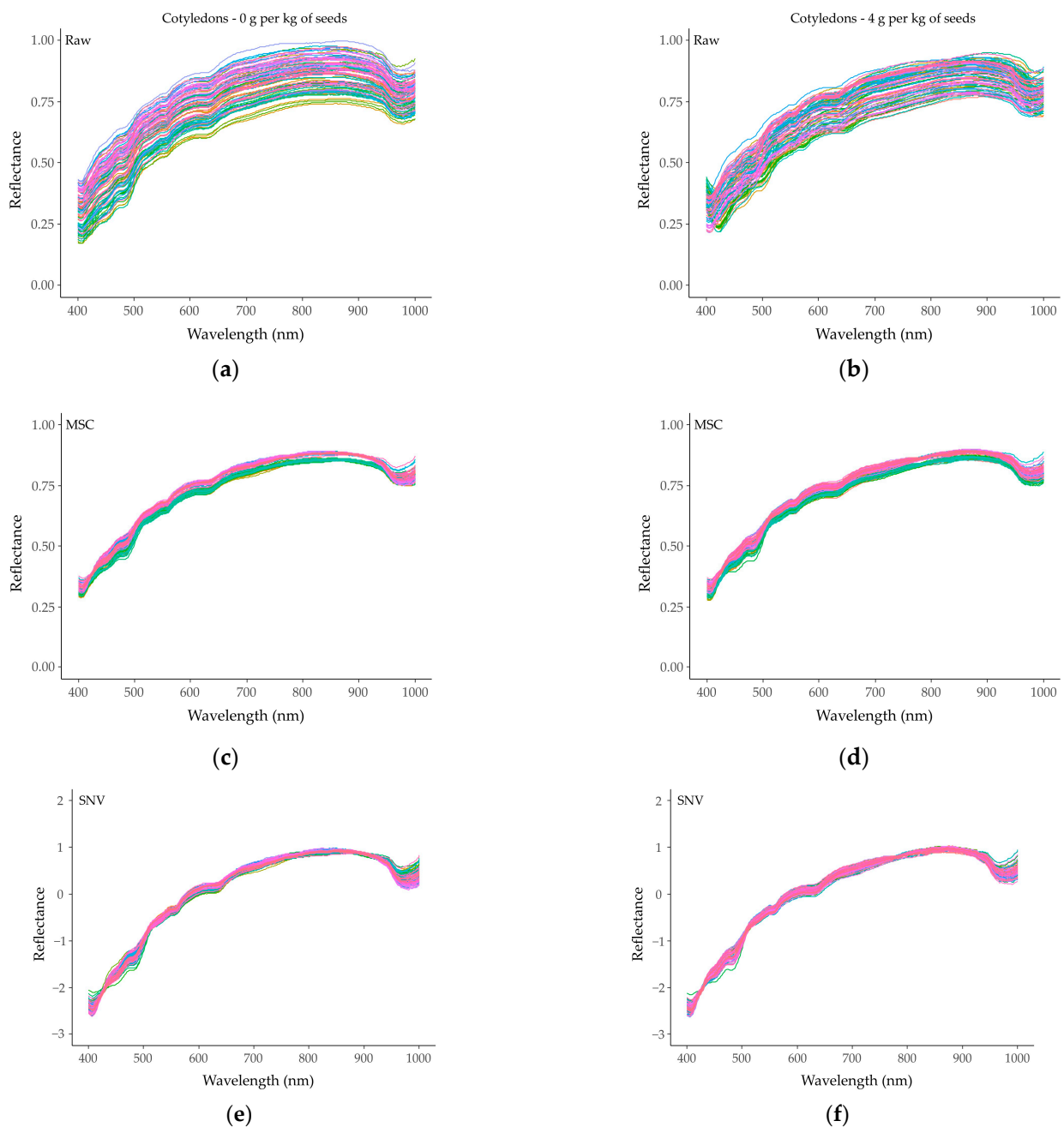


Figure 9. All spectral curves of untreated and micronutrient-treated soybean seeds subjected to different preprocessing methods: (a,b) raw spectra; (c,d) MSC processing; and (e,f) SNV processing of the cotyledons, respectively.

The raw and processed spectral curves obtained using the MSC and SNV methods in the embryonic axis region of the untreated and micronutrient-treated soybean seeds from the high- and low-vigor lots are shown in Figure 10a–f, respectively. It is observed that the application of MSC and SNV reduces the effect of light scattering in the original spectrum. The spectral behavior in the embryonic axis region of both the micronutrient-treated and untreated seeds is similar to that observed in the cotyledon region. Thus, it becomes necessary to extract and effectively use the spectral characteristics to establish a model capable of identifying seed vigor after micronutrient treatment.

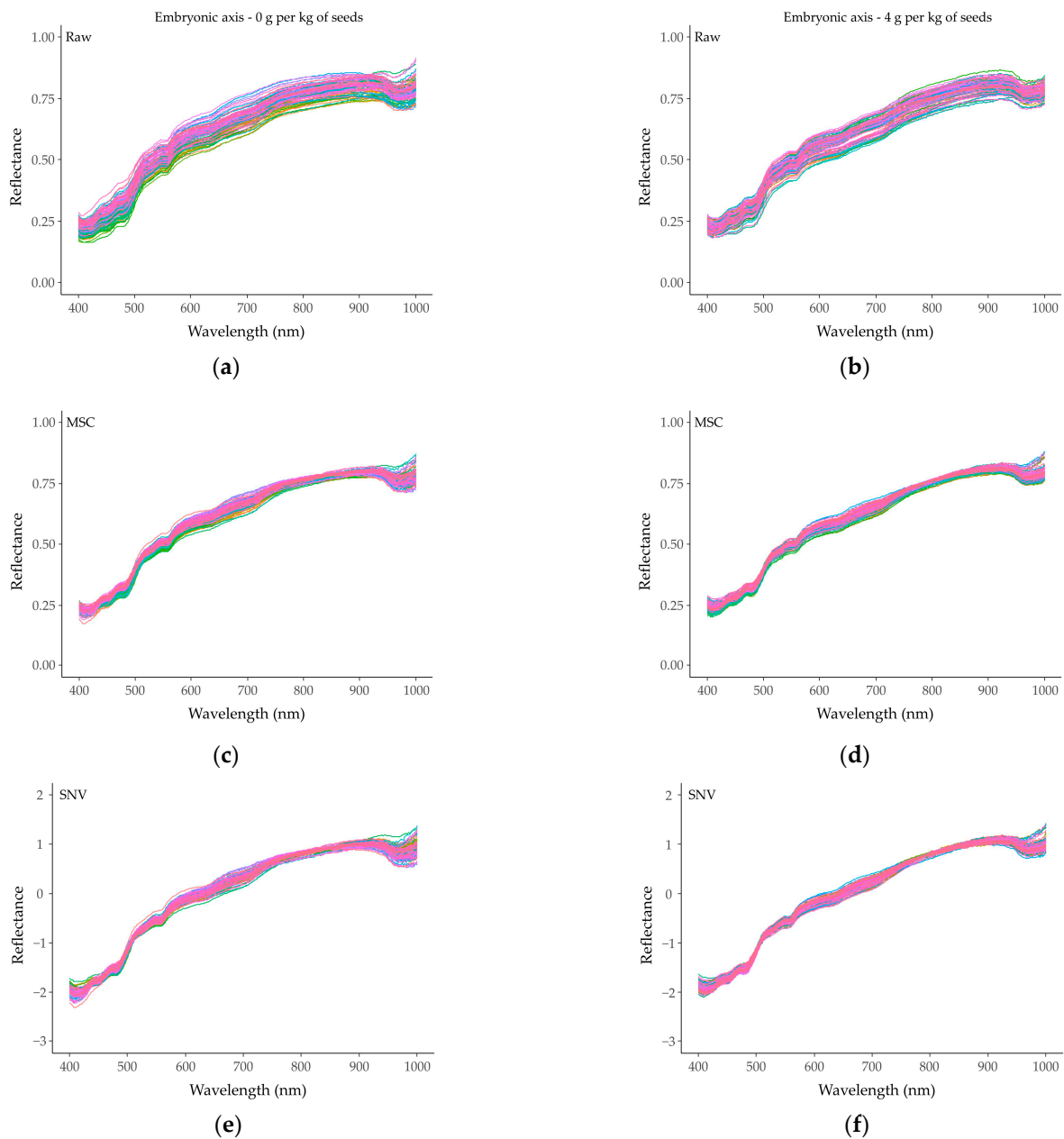


Figure 10. All spectral curves of untreated and micronutrient-treated soybean seeds subjected to different preprocessing methods: (a,b) raw spectra; (c,d) MSC processing; and (e,f) SNV processing of the embryonic axis region, respectively.

3.4. Optimal Wavelengths Selected via PCA

The results of the wavelengths selected via PCA of the raw and preprocessed spectral data of the cotyledon and embryonic axis region of the untreated seeds (0 g per kg of seeds) of the high- and low-vigor lots are shown in Table 1. The selected wavelengths in the cotyledon region exhibited similarity in the near-infrared range (863.57–890.00 nm) between the raw spectra and the MSC method. When the MSC and SNV preprocessing methods were applied, similarity was observed in the range of 943.24 to 952.16 nm. In the embryonic axis region, there was no similarity in the selected wavelengths between the raw data and the MSC preprocessing. However, the MSC and SNV methods shared a common visible-region wavelength (639.63 nm).

Table 1. Selected wavelengths from different regions of interest of seeds that were untreated and soaked for 20 h.

Region of Interest	Method of Preprocessing	Wavelength (nm)
Cotyledons	Raw	504.37; 506.42; 508.48; 859.17; 861.37; 863.57; 865.76; 867.96; 870.16; 872.36; 874.57; 876.77; 878.97; 881.18; 883.38; 885.59; 887.79; 890.00; 892.21; 894.42; 896.63; 898.84; 901.05; 903.26; 905.48; 907.69; 909.91 and 912.12.
	MSC	654.41; 656.53; 658.64; 660.76; 662.88; 665.00; 667.12; 863.57; 865.76; 867.96; 870.16; 872.36; 874.57; 876.77; 878.97; 881.18; 883.38; 885.59; 887.79; 890.00; 936.56; 938.78; 941.01; 943.24; 945.47; 947.7; 949.93 and 952.16.
	SNV	599.72; 601.81; 603.91; 606.00; 608.1; 610.19; 612.29; 614.39; 616.49; 943.24; 945.47; 947.7; 949.93; 952.16; 961.1; 965.57; 967.81; 970.04; 972.28; 974.52; 976.76; 979.01; 981.25; 983.49; 985.74; 987.98; 990.23 and 992.48.
Embryonic axis	Raw	539.4; 541.47; 543.53; 545.6; 547.67; 549.75; 551.82; 558.04; 560.12; 830.7; 835.07; 837.25; 839.44; 841.63; 843.82; 846.01; 848.2; 850.4; 852.59; 854.78; 856.98; 859.17; 861.37; 863.57; 865.76; 867.96; 870.16 and 872.36.
	MSC	633.31; 635.41; 637.52; 639.63; 641.74; 643.85; 645.96; 648.07; 650.18; 652.3; 654.41; 656.53; 658.64; 660.76; 662.88; 665.00; 667.12; 669.24; 673.48; 923.22; 925.44; 927.66; 929.88; 932.11; 934.33; 936.56; 938.78 and 941.01.
	SNV	606.00; 608.1; 610.19; 612.29; 614.39; 616.49; 618.59; 620.69; 622.79; 624.89; 626.99; 629.1; 631.2; 639.63; 795.85; 800.19; 802.36; 943.24; 974.52; 976.76; 979.01; 981.25; 983.49; 985.74; 987.98; 990.23; 992.48 and 996.97.

The specific wavelengths selected from the PCA of the raw and preprocessed spectral data from the region of the cotyledons and the embryonic axis of the treated seeds (4 g per kg of seeds) of the highest- and lowest-vigor lots are presented in Table 2. The raw extracted wavelengths from the cotyledon and embryonic axis regions did not correspond to the selected wavelengths from the MSC and SNV preprocessing methods. However, the selected characteristic bands from the preprocessing methods were consistent in both regions of interest and were within the visible spectral range, specifically, between 601.81 and 656.53 nm. It is evident that the cotyledon and embryonic axis regions of seeds that were untreated and treated with micronutrients from the high- and low-vigor lots exhibited different reflectance behaviors, which influenced the selected wavelength in the PCA analysis (Tables 1 and 2). The treated seeds showed a consistent relationship between the selected wavelengths, regardless of the analyzed region of interest, and the applied preprocessing method. However, the untreated seeds showed variation between the analyzed region and the spectral preprocessing method used.

Table 2. Selected wavelengths from different regions of interest of seeds treated with micronutrients and soaked for 20 h.

Region of Interest	Method of Preprocessing	Wavelength (nm)
Cotyledons	Raw	859.17; 861.37; 863.57; 865.76; 867.96; 870.16; 872.36; 874.57; 876.77; 878.97; 881.18; 883.38; 885.59; 887.79; 890.00; 892.21; 894.42; 896.63; 898.84; 901.05; 903.23; 905.48; 907.69; 909.91; 912.12; 914.34; 916.56 and 918.78.
	MSC	601.81; 608.1; 610.19; 612.29; 614.39; 616.49; 618.59; 620.69; 622.79; 624.89; 626.99; 629.1; 631.2; 633.31; 635.41; 637.52; 639.63; 641.74; 643.85; 645.96; 648.07; 650.18; 652.3; 654.41; 656.53; 658.64; 660.76 and 662.88.
	SNV	601.81; 610.19; 612.29; 614.39; 616.49; 618.59; 620.69; 622.79; 635.41; 637.52; 639.63; 641.74; 643.85; 645.96; 648.07; 650.18; 652.3; 654.41; 656.53; 934.33; 936.56; 938.78; 941.01; 943.24; 945.47; 947.7; 949.93 and 952.16.

Table 2. Cont.

Region of Interest	Method of Preprocessing	Wavelength (nm)
Embryonic axis	Raw	756.9; 759.06; 761.22; 763.38; 765.53; 767.69; 769.85; 772.02; 774.18; 776.34; 778.51; 780.67; 782.84; 785.00; 787.17; 789.34; 791.51; 793.68; 795.85; 798.02; 800.19; 802.36; 804.54; 806.71; 808.89; 811.07; 813.24 and 817.6.
	MSC	597.63; 599.72; 601.81; 603.91; 606.00; 608.1; 610.19; 612.29; 614.39; 616.49; 618.59; 620.69; 622.79; 624.89; 626.99; 629.1; 631.2; 633.31; 635.41; 637.52; 639.63; 641.74; 643.85; 645.96; 648.07; 932.11; 934.33 and 936.56.
	SNV	612.29; 614.39; 616.49; 618.59; 620.69; 622.79; 624.89; 626.99; 629.1; 631.2; 633.31; 635.41; 637.52; 639.63; 641.74; 970.04; 972.28; 974.52; 976.76; 979.01; 981.25; 983.49; 985.74; 987.98; 990.23; 992.48; 996.97 and 1000.

3.5. Models Based on Selected Bands

The accuracy of the classification models ANN, DT and PLS-DA, developed using spectral bands subjected to different preprocessing techniques and selected through PCA analysis of the cotyledon and embryonic axis regions of untreated soybean seeds, can be observed in Table 3. The use of MSC for the cotyledon region resulted in the highest classification accuracies of 88%, 86% and 100% for validation using the ANN, DT and PLS-DA models, respectively. Similar results were obtained for the embryonic axis region, which had a validation accuracy of 95% with ANN, 92% with DT and 100% with PLS-DA. The lowest classification accuracy in the cotyledon region of untreated seeds for both models was observed when using raw spectral bands, while for the embryonic axis region, the lowest classification accuracy for the ANN, DT and PLS-DA models was obtained with the application of the SNV preprocessing method. The results revealed that PLS-DA combined with the MSC preprocessing technique outperformed the other models, with the highest classification accuracy of 100% for both the cotyledon and embryonic axis regions of untreated seeds, respectively.

Table 3. Classification accuracy based on different models and preprocessing methods from different regions of interest of untreated seeds with different levels of vigor soaked for 20 h.

Region of Interest	Method of Preprocessing	Calibration Set (%)			Prediction Set (%)		
		ANN	DT	PLS-DA	ANN	DT	PLS-DA
Overall Accuracy (%)							
Cotyledons	Raw	97	70	100	53	65	68
	MSC	98	94	100	88	86	100
	SNV	100	100	100	83	81	89
Embryonic axis	Raw	100	84	93	76	85	90
	MSC	100	99	100	95	92	100
	SNV	98	97	80	54	66	73

ANN = artificial neural network, DT = decision tree and PLS-DA = partial least squares–discriminant analysis.

The best prediction performance for the classification models ANN and DT, developed using spectral bands extracted from the cotyledon and embryonic axis regions of micronutrient-treated soybean seeds, was achieved with the MSC preprocessing method (Table 4). On the other hand, the PLS-DA model showed higher classification performance using raw data for the cotyledon region (97%) and the preprocessing method for the embryonic axis region (100%). The PLS-DA model provided the highest classification accuracy of 97% and 100% for the cotyledon and embryonic axis regions, respectively, without considering the preprocessing methods. The lowest classification accuracy for the cotyledon and embryonic axis regions of treated seeds was observed with the SNV preprocessing method, regardless of the adopted classification model.

Table 4. Classification accuracy based on different models and preprocessing methods from different regions of interest of seeds with different levels of vigor treated and soaked for 20 h.

Region of Interest	Method of Preprocessing	Calibration Set			Prediction Set		
		Overall Accuracy (%)					
		ANN	DT	PLS-DA	ANN	DT	PLS-DA
Cotyledons	Raw	94	92	100	86	73	97
	MSC	100	96	93	90	88	92
	SNV	100	96	98	33	46	38
Embryonic axis	Raw	98	100	98	43	50	41
	MSC	100	100	100	92	85	100
	SNV	98	100	96	30	38	41

ANN = artificial neural network, DT = decision tree and PLS-DA = partial least squares–discriminant analysis.

4. Discussion

Evaluations conducted during the initial characterization of seed lots are routinely used in seed quality control laboratories to assess seed viability and vigor. The germination test aims to determine the maximum germination capacity of a seed lot under ideal conditions, taking into account the formation of normal seedlings. The first germination count is an auxiliary test to the germination test, which allows for the observation of the speed of normal seedling formation. The accelerated aging test evaluates the performance of seeds after being subjected to stress conditions such as high temperature and relative humidity. The tetrazolium test, on the other hand, is based on the respiratory activity of cells composing the seed tissues. In the tetrazolium test, the seed quality is determined by identifying problems that occurred in the field. Analysis of the emergence of seedlings in the field is a vigor test that assesses the performance of seedlings under field conditions, and it is the test that most closely represents the reality faced by the producer, as it allows the observation of plant establishment in the field. The vigor of the lots, as evaluated through the tests, allowed for characterization of the lots in this research as having high or low vigor.

These tests are essential for seed quality control, providing important information about viability and vigor. They assist in making decisions regarding seed storage, commercialization and sowing. The vigor of seeds is a decisive factor for agricultural production, and the use of micronutrients applied through seeds can be influenced by the vigor level. Less vigorous seeds are more susceptible to phytotoxicity [26]. According to Bewley et al. [27], seeds with high vigor require less time to complete their initial DNA repair, which promotes tolerance to stressful conditions. Seedling emergence is directly related to seed vigor, with lots composed of more vigorous seeds resulting in faster and more uniform emergence [3,28]. Therefore, understanding the physiological potential of seed lots and the effect of seed treatment with micronutrients needs to be further clarified.

The absorption of water by seeds is a three-phase process. Phase I of the water absorption process in seeds is characterized by rapid water uptake and the reactivation of metabolism, mainly involving membrane and DNA repair activities. In Phase II, there is a reduction in the rate of water absorption, and the main events are related to cell elongation preparation, particularly in the radicle. Phase III is characterized by the resumption of the growth of the embryonic axis and the emergence of the primary root. In this phase, the mobilized reserves are transported to be assimilated by the growing points of the embryo, leading to the growth of the seedling [27]. According to Marcos-Filho et al. [29], water uptake during the seed hydration process for a period of eight to sixteen hours triggers the first signs of metabolic reactivation, including increased respiratory activity and energy availability for germination, enzyme activation and protein synthesis. Therefore, the 20 h period adopted in this study would be suitable for analyzing the absorption and mobilization of micronutrients by soybean seeds from high- and low-vigor lots.

The X-ray fluorescence (XRF) technique is an important tool for assessing nutrient distribution in seeds [30]. However, the low concentration of micronutrients in seed tissues makes their quantification challenging. In a study by Romeu et al. [7], XRF analysis was used to investigate the elemental distribution in soybean seeds before and during germination. The researchers also did not identify the presence of Mo and attributed it to its low concentration. Soybean seeds have a natural concentration of micronutrients that can vary depending on the specific micronutrient. In a study by Magalhães et al. [31], the concentration of mineral nutrients was quantified in seeds of three soybean cultivars (TMG 132, P98Y11 and NS 8270). The researchers found that the accumulation of micronutrients in the seeds followed the order Zn, Mn and Cu, respectively, for all three cultivars studied, which is consistent with the findings of the present research. It is worth noting that seed vigor also affects the concentration of micronutrients, as seeds with high vigor have a high concentration of Zn and Mn compared to those with low vigor.

The higher concentration of Zn and Mn found in soybeans is probably associated with the role of these micronutrients during germination and initial seedling development. Zn plays a crucial role in the biosynthesis of enzymes and proteins involved in various metabolic activities [32], while Mn is involved in multiple processes throughout the plant's life cycle, including photosynthesis, respiration and the elimination of reactive oxygen species [33]. Thus, it becomes evident that micronutrient concentration contributes to seed vigor, with more vigorous seeds establishing themselves rapidly and uniformly under different environmental conditions.

The absorption of micronutrients applied individually or in combination through seed treatment still raises uncertainty in the scientific community. The results obtained show that regardless of seed vigor, the highest concentration of micronutrients (Cu, Zn and Mn) is found in the hilum and seed coat region, which is in agreement with previous findings for soybean seeds using the μ -XRF technique to analyze zinc absorption [9,34], copper, molybdenum, zinc [8] and nickel [35]. However, these same authors mention that micronutrients applied via seed treatment will later be transferred to the rhizosphere soil and ultimately absorbed by the roots.

This research is pioneering in the use of hyperspectral imaging to evaluate seed tissues with different levels of vigor treated with micronutrients. The reflectance of untreated seeds with low vigor was high compared to seeds with high vigor. Seeds with low vigor exhibit a more pronounced deterioration process, which causes damage to membrane systems, lipid peroxidation, and higher electrolyte leakage. The absorption peaks between 600–800 nm are primarily related to the lipid content in soybean seeds, where higher lipid content leads to higher reflectance [18]. The cotyledon and embryonic axis regions of micronutrient-treated seeds did not show differences in reflectance related to vigor level. The seed coat is a protective structure between the embryo and the external environment, composed of layers of cells with thick walls. The presence of micronutrients in the seed coat may have influenced the water absorption dynamics, affecting reflectance.

In the NIR region between 760–1070 nm, primarily the harmonics and combinations of fundamental vibrations of the functional groups OH, NH, and CH are produced. These functional groups are essential components of seed molecules such as carbohydrates, fats, water and proteins. Consequently, the types/structures and concentrations of molecules in seeds have a significant impact on spectral information [36]. Therefore, the observed behavior of higher reflectance in untreated seeds with low vigor compared to seeds with high vigor is associated with a more pronounced deterioration process, which primarily leads to reduced water absorption and modifications in the seed membrane system (Figure 8a,c).

To select the best preprocessing methods for reducing noise interference in spectral data, different preprocessing methods were applied. The results showed that the MSC method was the most appropriate for preprocessing the spectral information obtained from the cotyledon and embryonic axis regions of both high- and low-vigor soybean seeds that were untreated and treated with micronutrients (Tables 3 and 4). The MSC preprocessing method attenuates the effect of light scattering in the original spectrum, thereby increasing

the accuracy of the model. It has been previously used in research studies that aimed to detect seed vigor, as demonstrated by [24,37]. In this study, we applied a machine learning approach based on classification models to verify whether it is possible to identify the vigor of soybean seeds before and after treatment with micronutrients. We obtained satisfactory classification results for vigor discrimination, and the results are in line with those obtained through XRF and μ -XRF techniques.

The HSI technique has shown promise for investigating the metabolism of micronutrient absorption in soybean seeds. Future studies using wider ranges of the electromagnetic spectrum, considering, for example, the entire infrared region, may yield important results related to protein, lipid and starch metabolism in response to seed treatment with micronutrients or other elements, particularly when seeds with different levels of vigor are used. Therefore, the integration of spectral data and X-ray fluorescence data assisted in explaining the dynamics of micronutrient absorption applied via seed treatment with different levels of vigor.

5. Conclusions

The technique of X-ray fluorescence spectroscopy identified higher concentrations of micronutrients in the treated seeds, with zinc being the predominant element. Microprobe X-ray fluorescence spectroscopy analysis revealed that a significant proportion of the micronutrients remained adhered to the hilum and seed coat, irrespective of seed vigor.

The PLS-DA classification model using spectral data exhibited higher accuracy in classifying soybean seeds with high and low vigor, regardless of seed treatment with micronutrients and the analyzed region.

Author Contributions: Conceptualization, R.M.A. and F.G.G.-J.; methodology, R.M.A., F.H.I.-F., A.d.S.C.-F., G.d.F.R.R. and C.H.Q.R.; formal analysis, R.M.A. and C.H.Q.R.; investigation, R.M.A. and A.d.S.C.-F.; resources, F.G.G.-J. and P.T.Y.; data curation, R.M.A. and C.H.Q.R.; writing—original draft preparation, R.M.A. and F.G.G.-J.; writing review and editing, R.M.A., F.G.G.-J., A.d.S.C.-F., G.d.F.R.R., C.H.Q.R., F.H.I.-F. and P.T.Y.; supervision, F.G.G.-J. and P.T.Y.; project administration, F.G.G.-J. and P.T.Y.; funding acquisition, F.G.G.-J. and P.T.Y. All authors have read and agreed to the published version of the manuscript.

Funding: This research was funded by the “Luiz de Queiroz” Agrarian Studies Foundation (FEALQ); by the National Council for Scientific and Technological Development (CNPq), No. 130734/2020-9; and by the São Paulo Research Foundation (FAPESP), No. 2018/13139-0 and No. 2018/02317-5.

Data Availability Statement: Not available.

Acknowledgments: The authors thank the graduate program in Crop Science at ESALQ/USP and the companies Lagoa Bonita Sementes and Nutrien Ltd.

Conflicts of Interest: The authors declare no conflict of interest.

References

1. Saito, Y.; Itakura, K.; Kuramoto, M.; Kaho, T.; Ohtake, N.; Hasegawa, H.; Suzuki, T.; Kondo, N. Prediction of protein and oil contents in soybeans using fluorescence excitation emission matrix. *Food Chem.* **2021**, *365*, 130403. [[CrossRef](#)] [[PubMed](#)]
2. Cattelan, A.J.; Dall’Agnol, A. The rapid soybean growth in Brazil. *Oilseeds Fats Crop. Lipids* **2018**, *25*, 58. [[CrossRef](#)]
3. Ebone, L.A.; Caverzan, A.; Tagliari, A.; Chiomento, J.L.T.; Silveira, D.C.; Chavarria, G. Soybean seed vigor: Uniformity and growth as key factors to improve yield. *Agronomy* **2020**, *10*, 545. [[CrossRef](#)]
4. Finch-Savage, W.E.; Bassel, G.W. Seed vigour and crop establishment: Extending performance beyond adaptation. *J. Exp. Bot.* **2016**, *67*, 567–591. [[CrossRef](#)]
5. Hansel, F.D.; Oliveira, M.L. *Importance of Micronutrients in Soybean Culture in Brazil*; International Plant Nutrition Institute: Piracicaba, Brazil, 2016.
6. Bhat, B.A.; Islam, S.T.; Ali, A.; Sheikh, B.A.; Tariq, L.; Islam, S.U.; Hassan Dar, T.U. Role of micronutrients in secondary metabolism of plants. *Plant Micronutr.* **2020**, *13*, 311–329. [[CrossRef](#)]
7. Romeu, S.L.Z.; Marques, J.P.R.; Montanha, G.S.; de Carvalho, H.W.P.; Pereira, F.M.V. Chemometrics unraveling nutrient dynamics during soybean seed germination. *Microchem. J.* **2021**, *164*, 106045. [[CrossRef](#)]

8. Montanha, G.S.; Dias, M.A.N.; Corrêa, C.G.; de Carvalho, H.W.P. Unfolding the fate and effects of micronutrients supplied to soybean (*Glycine max* (L.) Merrill) and maize (*Zea mays* L.) through seed treatment. *J. Soil Sci. Plant Nutr.* **2021**, *21*, 3194–3202. [[CrossRef](#)]
9. Rohr, L.A.; França-Silva, F.; Corrêa, C.G.; de Carvalho, H.W.P.; Gomes-Junior, F.G. Soybean seeds treated with zinc evaluated by X-ray micro-fluorescence spectroscopy. *Sci. Agric.* **2023**, *80*, e20210131. [[CrossRef](#)]
10. Amigo, J.M.; Martí, I.; Gowen, A. Hyperspectral Imaging and Chemometrics. A perfect combination for the analysis of food structure, composition and quality. *Data Handl. Sci. Technol.* **2013**, *28*, 343–370. [[CrossRef](#)]
11. Elmasry, G.; Mandour, N.; Al-Rejaie, S.; Belin, E.; Rousseau, D. Recent applications of multispectral imaging in seed phenotyping and quality monitoring-an overview. *Sensors* **2019**, *19*, 1090. [[CrossRef](#)]
12. Amigo, J.M.; Babamoradi, H.; Elcoroaristizabal, S. Hyperspectral Image analysis. A Tutorial. *Anal. Chim. Acta* **2015**, *896*, 34–51. [[CrossRef](#)] [[PubMed](#)]
13. Kemsley, E.K.; Defernez, M.; Marini, F. Multivariate statistics: Considerations and confidences in food authenticity problems. *Food Control* **2019**, *105*, 102–112. [[CrossRef](#)]
14. Li, Y.; Sun, J.; Wu, X.; Chen, Q.; Lu, B.; Dai, C. Detection of viability of soybean seed based on fluorescence hyperspectra and CARS-SVM-AdaBoost model. *J. Food Process. Preserv.* **2019**, *43*, e14238. [[CrossRef](#)]
15. Zhu, S.; Chao, M.; Zhang, J.; Xu, X.; Song, P.; Zhang, J.; Huang, Z. Identification of soybean seed varieties based on hyperspectral imaging technology. *Sensors* **2019**, *19*, 5225. [[CrossRef](#)] [[PubMed](#)]
16. Fu, D.; Zhou, J.; Scaboo, A.M.; Niu, X. Nondestructive phenotyping fatty acid trait of single soybean seeds using reflective hyperspectral imagery. *J. Food Process Eng.* **2021**, *44*, e13759. [[CrossRef](#)]
17. Aulia, R.; Kim, Y.; Zuhrotul Amanah, H.; Muhammad Akbar Andi, A.; Kim, H.; Kim, H.; Lee, W.H.; Kim, K.H.; Baek, J.H.; Cho, B.K. Non-Destructive prediction of protein contents of soybean seeds using near-Infrared Hyperspectral Imaging. *Infrared Phys. Technol.* **2022**, *127*, 104365. [[CrossRef](#)]
18. Yang, Y.; Liao, J.; Li, H.; Tan, K.; Zhang, X. Identification of high-oil content soybean using hyperspectral reflectance and one-dimensional convolutional neural network. *Spectrosc. Lett.* **2023**, *56*, 28–41. [[CrossRef](#)]
19. Guo, Z.; Zhang, J.; Ma, C.; Yin, X.; Guo, Y.; Sun, X.; Jin, C. Application of visible-near-infrared hyperspectral imaging technology coupled with wavelength selection algorithm for rapid determination of moisture content of soybean seeds. *J. Food Compos. Anal.* **2023**, *116*, 105048. [[CrossRef](#)]
20. Ministério da Agricultura, Pecuária e Abastecimento. *Regras Para Análise de Sementes*; Ministério da Agricultura, Pecuária e Abastecimento: Brasília, Brasil, 2009.
21. Krzyzanowski, F.C.; Vieira, R.D.; França-Neto, J.B.; Marcos-Filho, J. *Vigor de Sementes: Conceitos e Testes*, 2nd ed.; ABRATES: Londrina, Brazil, 2020.
22. Almeida, E.; Montanha, G.S.; Carvalho, H.W.P.; Marguí, E. Evaluation of energy dispersive X-ray fluorescence and total reflection X-ray fluorescence spectrometry for vegetal mass-limited sample analysis: Application to soybean root and shoots. *Spectrochim. Acta* **2020**, *170*, 105915. [[CrossRef](#)]
23. R Core Team. *R: A Language and Environment for Statistical Computing*; R Foundation for Statistical Computing: Vienna, Austria, 2020. Available online: <https://www.R-project.org/> (accessed on 1 May 2023).
24. Xu, P.; Sun, W.; Xu, K.; Zhang, Y.; Tan, Q.; Qing, Y.; Yang, R. Identification of defective maize seeds using hyperspectral imaging combined with deep learning. *Foods* **2023**, *12*, 144. [[CrossRef](#)]
25. Bian, X.; Wang, K.; Tan, E.; Diwu, P.; Zhang, F.; Guo, Y. A selective ensemble preprocessing strategy for near-infrared spectral quantitative analysis of complex samples. *Chemom. Intell. Lab. Syst.* **2020**, *197*, 103916. [[CrossRef](#)]
26. Bakhshandeh, E.; Gholamhossieni, M. Quantification of soybean seed germination response to seed deterioration under peg-induced water stress using hydrotime concept. *Acta Physiol. Plant.* **2018**, *40*, 126. [[CrossRef](#)]
27. Bewley, J.D.; Bradford, K.J.; Hilhorst, W.M.H.; Nonogaki, H. *Seeds: Physiology of Development, Germination and Dormancy*, 3rd ed.; Springer Science & Business Media: New York, NY, USA, 2012; ISBN 9781461446927.
28. Rossi, R.F.; Cavariani, C.; França-Neto, J.d.B. Seed vigor, plant population and agronomic performance of soybean. *Rev. Ciênc. Agrar.-Amaz. J. Agric. Environ. Sci.* **2017**, *60*, 215–222. [[CrossRef](#)]
29. Marcos-Filho, J. *Seed Physiology of Cultivated Plants*, 2nd ed.; ABRATES: Londrina, Brazil, 2015.
30. Montanha, G.S.; Romeu, S.L.Z.; Marques, J.P.R.; Rohr, L.A.; De Almeida, E.; Dos Reis, A.R.; Linhares, F.S.; Sabatini, S.; De Carvalho, H.W.P. Microprobe-XRF assessment of nutrient distribution in soybean, cowpea, and kidney bean seeds: A fabaceae family case study. *ACS Agric. Sci. Technol.* **2022**, *2*, 1318–1324. [[CrossRef](#)]
31. Magalhães, W.d.A.; Megaioli, T.G.; Freddi, O.d.S.; Santos, M.A. Nutrient quantification in soybeans. *Rev. Ciênc. Agroambient.* **2015**, *13*, 95–100.
32. Singh, A.; Singh, N.B.; Afzal, S.; Singh, T.; Hussain, I. Zinc Oxide Nanoparticles: A review of their biological synthesis, antimicrobial activity, uptake, translocation and biotransformation in plants. *J. Mater. Sci.* **2018**, *53*, 185–201. [[CrossRef](#)]
33. Alejandro, S.; Höller, S.; Meier, B.; Peiter, E. Manganese in plants: From acquisition to subcellular allocation. *Front. Plant Sci.* **2020**, *11*, 300. [[CrossRef](#)]
34. Montanha, G.S.; Rodrigues, E.S.; Marques, J.P.R.; de Almeida, E.; Colzato, M.; Pereira de Carvalho, H.W. Zinc Nanocoated Seeds: An Alternative to Boost Soybean Seed Germination and Seedling Development. *SN Appl. Sci.* **2020**, *2*, 857. [[CrossRef](#)]

35. Oliveira, J.B.d.; Rodrigues Marques, J.P.; Rodak, B.W.; Galindo, F.S.; Carr, N.F.; Almeida, E.; Araki, K.; Gonçalves, J.M.; Rodrigues dos Reis, A.; van der Ent, A.; et al. Fate of nickel in soybean seeds dressed with different forms of nickel. *Rhizosphere* **2022**, *21*, 100464. [[CrossRef](#)]
36. Zhang, T.; Lu, L.; Yang, N.; Fisk, I.D.; Wei, W.; Wang, L.; Li, J.; Sun, Q.; Zeng, R. Integration of hyperspectral imaging, non-targeted metabolomics and machine learning for vigour prediction of naturally and accelerated aged sweetcorn seeds. *Food Control* **2023**, *153*, 109930. [[CrossRef](#)]
37. Cheng, T.; Chen, G.; Wang, Z.; Hu, R.; She, B.; Pan, Z.; Zhou, X.-G.; Zhang, G.; Zhang, D. Hyperspectral and imagery integrated analysis for vegetable seed vigor detection. *Infrared Phys. Technol.* **2023**, *131*, 104605. [[CrossRef](#)]

Disclaimer/Publisher's Note: The statements, opinions and data contained in all publications are solely those of the individual author(s) and contributor(s) and not of MDPI and/or the editor(s). MDPI and/or the editor(s) disclaim responsibility for any injury to people or property resulting from any ideas, methods, instructions or products referred to in the content.